SUPPLEMENTAL MATERIAL

Supplemental Figures and Figure Legends

TGFβ1 inhibits pseudoaneurysm formation after aortic patch angioplasty

Hualong Bai, Jung Seok Lee, Haidi Hu, Tun Wang, Toshihiko Isaji,
Shirley Liu, Jianming Guo, Haiyang Liu, Katharine Wolf, Shun Ono, Xiangjiang Guo,
Bogdan Yatsula, Ying Xing, Tarek M. Fahmy, Alan Dardik

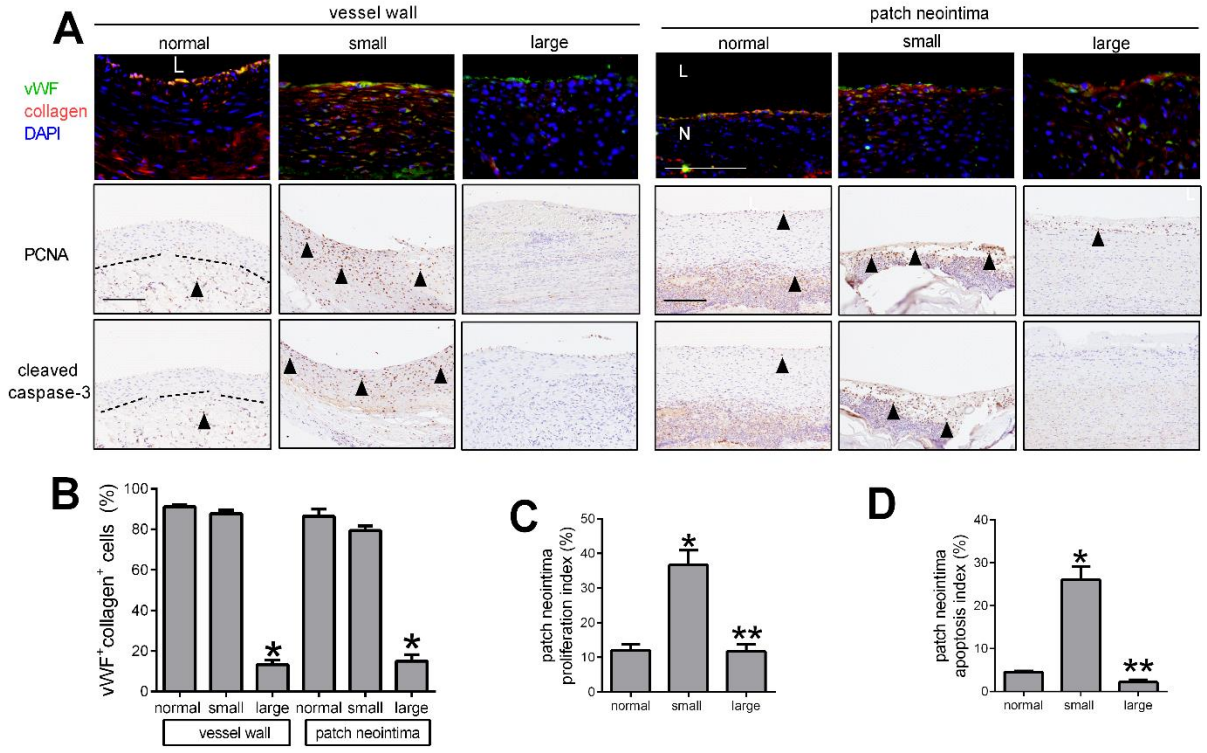

Supplementary Figure I: Proliferation and apoptosis in normal healing vessels and small and large pseudoaneurysms. A) First row, immunofluorescence analysis of the vessel wall and patch neointima in the rat aorta patch angioplasty at day 30, merge of vWF (green), collagen (red) and DAPI (blue); second row, immunohistochemistry stained for PCNA, arrowheads show the positive cells; third row, immunohistochemistry stained for cleaved caspase-3, arrowheads show the positive cells; dashed line shows the demarcation of the media and adventitia; scale bar, 100 µm; n=2-5. **B)** Bar graphs showing wWF and collagen dual positive cells in the vessel wall ($p<0.0001$, ANOVA; *, $p<0.0001$, vs. normal and small; Tukey's multiple comparisons test) and neointima ($p<0.0001$, ANOVA; *, $p<0.0001$, vs. normal and small; Tukey's multiple comparisons test); n=2-5. **C)** Bar graph showing the proliferation index in the patch neointima ($p=0.0014$, ANOVA; *, $p=0.0025$, vs. normal; **, $p=0.0023$, vs. small; Tukey's multiple comparisons test); n=3. **D)** Bar graph showing the apoptosis index in the patch neointima ($p=0.0002$, ANOVA; *, $p=0.0004$, vs. normal; **, $p=0.0004$, vs. small; Tukey's multiple comparisons test); n=2-5.

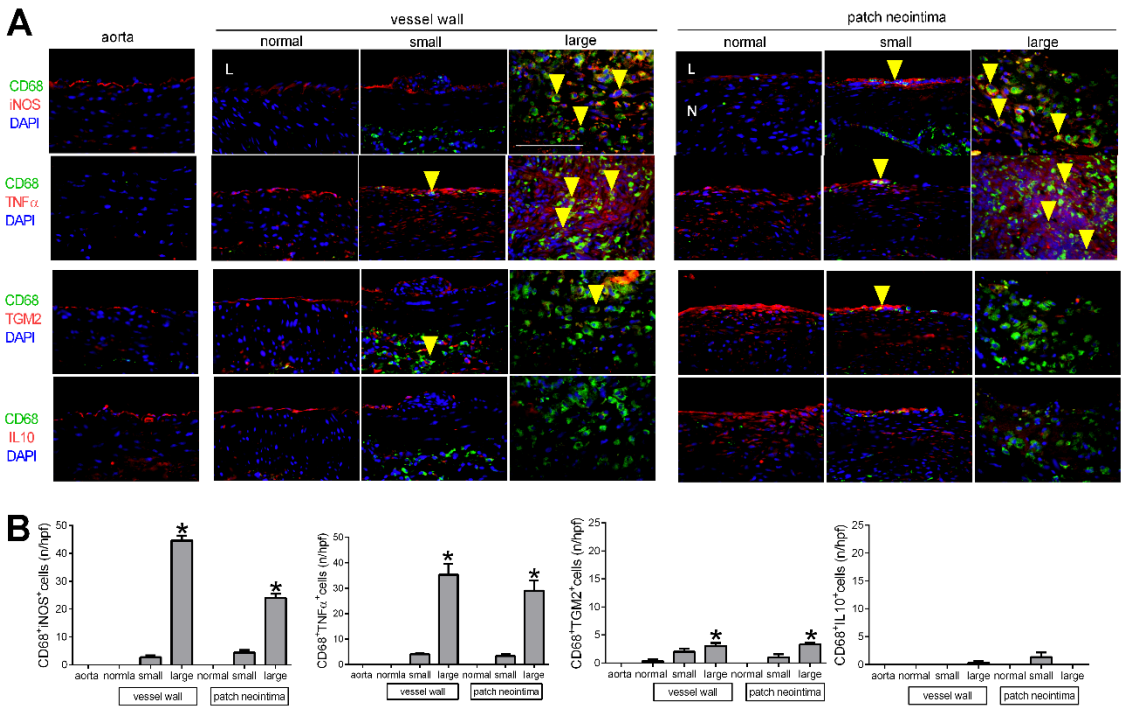

Supplementary figure II: Presence of macrophages after patch angioplasty. A) Immunofluorescence analysis of the vessel wall and patch neointima after rat aorta patch angioplasty, day 30; first row, merge of CD68 (green), iNOS (red) and DAPI (blue); second row, merge of CD68 (green), TNF α (red) and DAPI (blue); third row, merge of CD68 (green), TGM2 (red) and DAPI (blue); fourth row, merge of α-CD68 (green), IL10 (red) and DAPI (blue); N, neointima; L, lumen; yellow arrows showing the dual positive cells; scale bar, 100 µm; n=2-5. **B)** Bar graphs showing CD68 and iNOS dual positive cells in the vessel wall ($p<0.0001$, ANOVA; *, $p<0.0001$, vs. normal and small; Tukey's multiple comparisons test) and patch neointima ($p<0.0001$, ANOVA; *, $p<0.0001$, vs. normal and small; Tukey's multiple comparisons test); CD68 and TNF α dual positive cells in the vessel wall ($p=0.0001$, ANOVA; *, $p<0.0002$, vs. normal and small; Tukey's multiple comparisons test) and patch neointima ($p=0.0003$, ANOVA; *, $p<0.0004$, vs. normal and small; Tukey's multiple comparisons test); CD68 and TGM2 dual positive cells in the vessel wall ($p=0.0027$, ANOVA; *, $p=0.0234$, vs. normal healing; Tukey's multiple comparisons test) and patch neointima ($p=0.0023$, ANOVA; *, $p<0.0022$, vs. normal healing and small; Tukey's multiple comparisons test); and CD68 and IL 10 dual positive cells in the vessel wall ($p=0.4219$, ANOVA) and patch neointima ($p=0.1828$, ANOVA); n=2-5.

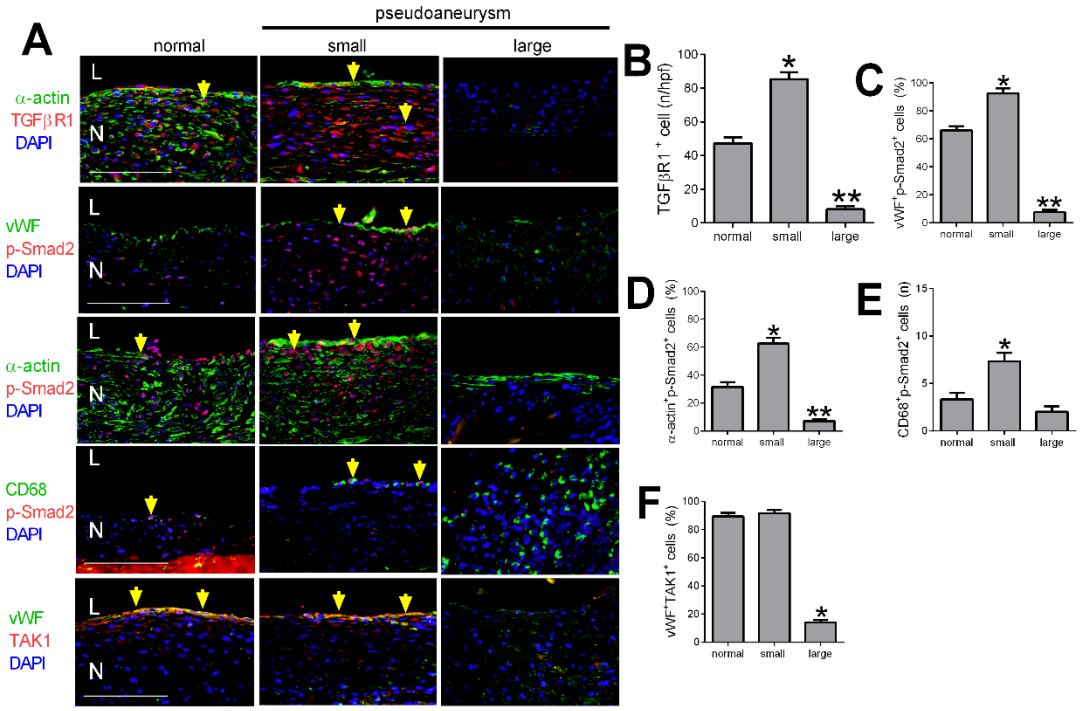

Supplementary Figure III: TGFβ signaling pathway in the neointima after patch angioplasty. A) Immunofluorescence of the neointima of the normal healing, small and large pseudoaneurysm; first row, merge of TGFβR1 (red), α-actin (green) and DAPI (blue); second row, merge of vWF (green), p-smad2 (green) and DAPI (blue); third row, merge of α-actin (green), p-smad2 (red) and DAPI (blue); fourth row, merge of CD68 (green), p-smad2 (red) and DAPI (blue); fifth row, merge of vWF (green), TAK1 (red) and DAPI (blue); L, lumen; N, neointima; yellow arrow showing the dual positive cells; scale bar, 100 µm; n=2-5. **B)** Bar graph showing number of TGFβR1-/α-actin- dual positive cells in the neointima ($p<0.0001$, ANOVA; *, $p=0.0005$, vs. normal; **, $p<0.0001$, vs. small; Tukey's multiple comparisons test); n=2-5. **C)** Bar graph showing vWF and p-Smad2 dual positive cells in the neointima ($p<0.0001$, ANOVA; *, $p=0.0045$, vs. small; **, $p<0.0001$, vs. small; Tukey's multiple comparisons test); n=2-5. **D)** Bar graph showing α-actin and p-smad2 dual positive cells in the neointima ($p=0.0001$, ANOVA; *, $p=0.0031$, vs. normal; **, $p=0.0001$, vs. small; Tukey's multiple comparisons test); n=2-5. **E)** Bar graph showing CD68 and p-smad2 dual positive cells in the neointima ($p=0.0047$, ANOVA; *, $p<0.018$, vs. normal and large; Tukey's multiple comparisons test); n=2-5. **F)** Bar graph showing vWF and TAK1 dual positive cells in the neointima ($p<0.0001$, ANOVA; *, $p<0.0001$, vs. normal and small; Tukey's multiple comparisons test); n=2-5.

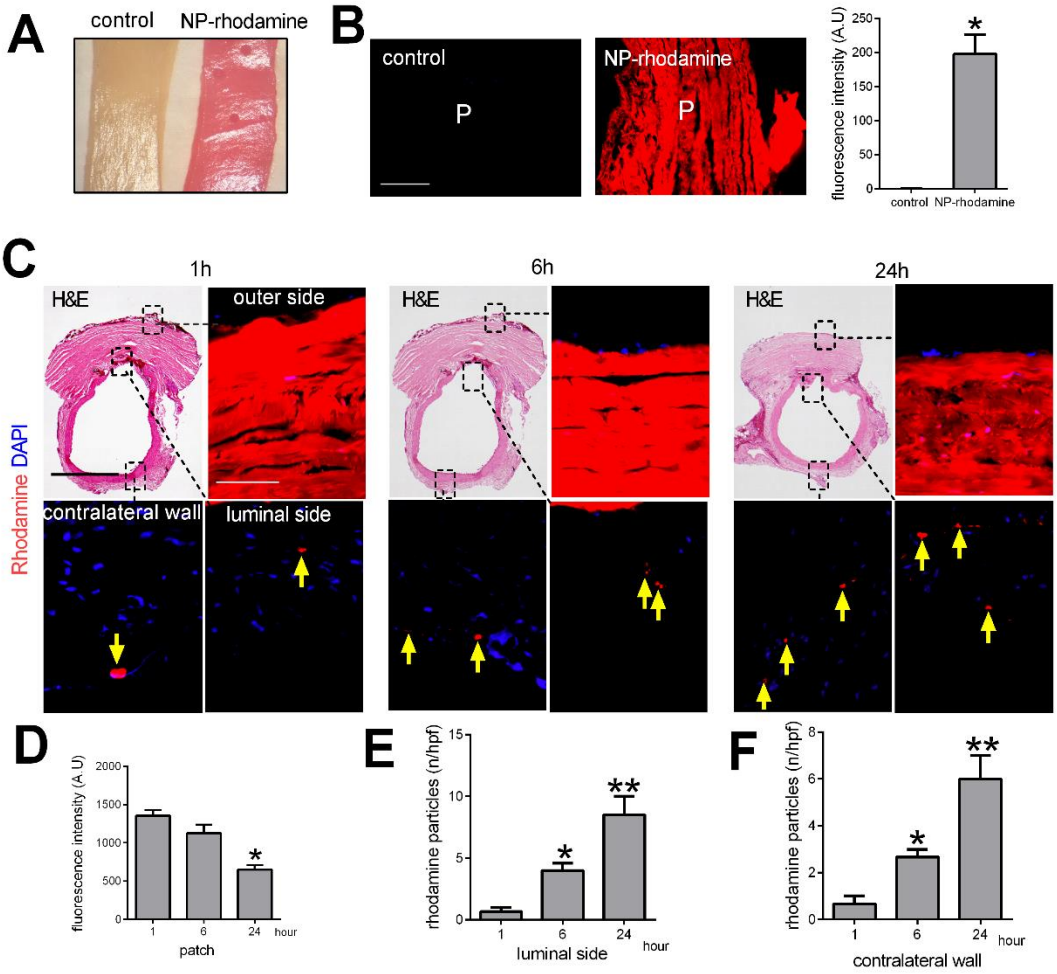

Supplementary Figure IV: Detection of rhodamine in the aortic wall. A) Light microscope comparison of pericardial patch before and after nanoparticle rhodamine conjugation. **B)** Immunofluorescence photographs before and after nanoparticle rhodamine conjugation; scale bar, 200 µm; P, patch; n=3. Bar graph shows the immunofluorescence intensity of nanoparticles (*, p=0.0022; t-test); n=3. **C)** Nanoparticle rhodamine release after nanoparticle rhodamine conjugated patch angioplasty in rat aorta at 1 h, 6 h and 24 h; the dashed rectangles and lines in the hematoxylin and eosin (H&E) photograph show the outer and luminal sides of the patch and contralateral aortic wall facing the patch; yellow arrows show the rhodamine auto fluorescence; DAPI, blue; scale bar, H&E, 0.5 mm; immunofluorescence photos, 50 µm; n=3. **D)** Bar graph showing the fluorescence intensity of rhodamine particles on the patch luminal side (p=0.0031, ANOVA; *, p<0.02, vs. 1 h, 6 h; Tukey's multiple comparisons test); n=3. **E)** Bar graph showing the number of rhodamine particles on the patch luminal side (p=0.0001, ANOVA; *, p=0.0368 vs. 1 h; **, p=0.0048 vs. 6 h; Tukey's multiple comparisons test); n=3. **F)** Bar graph showing the number of rhodamine particles on the contralateral aortic wall (p=0.0001, ANOVA; *, p=0.0201 vs. 1 h; **, p=0.0076 vs. 6 h; Tukey's multiple comparisons test); n=3.

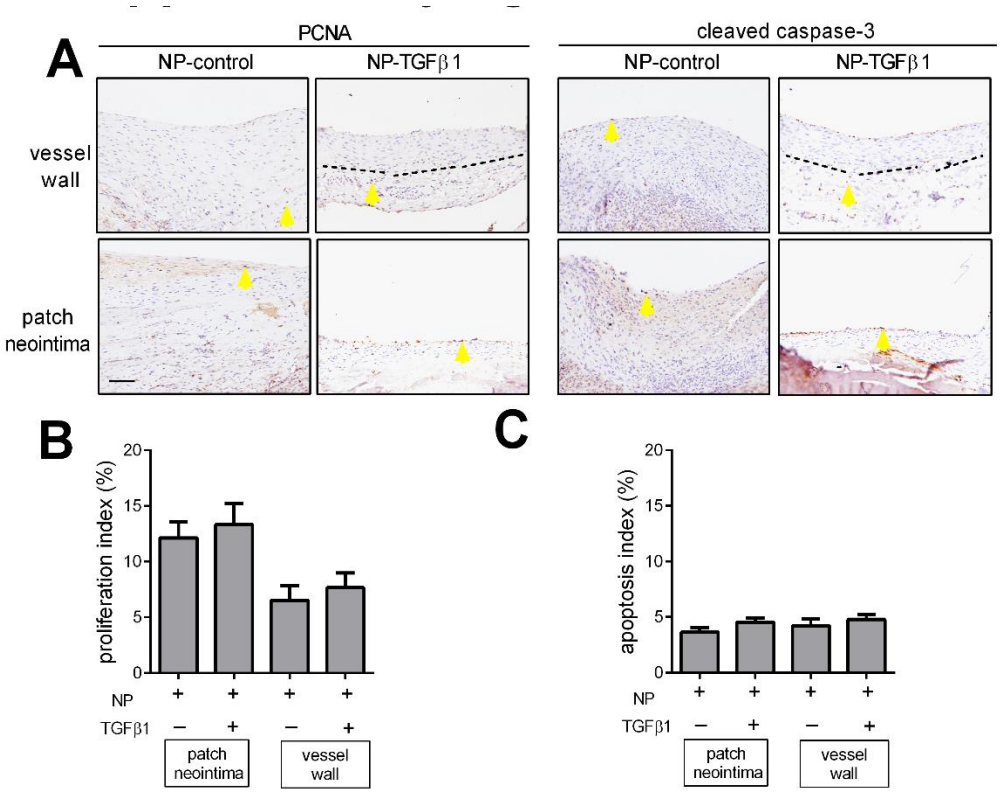

Supplementary Figure V: Proliferation and apoptosis with TGFβ1 delivery. A) Immunohistochemistry stained with PCNA (left panel) and cleaved caspase-3 (right panel) in NP-control and NP-TGFβ1 groups; arrows show the positive cells; dashed line shows the demarcation of the media and adventitia; n=4-6. **B)** Bar graph showing the proliferation index in the patch neointima (p=0.6383, t-test) and vessel wall (p=0.5747, t-test); n=4-6. **C)** Bar graph showing the apoptosis index in the patch neointima (p=0.2057, t-test) and vessel wall (p=0.5308, t-test); n=4-6.

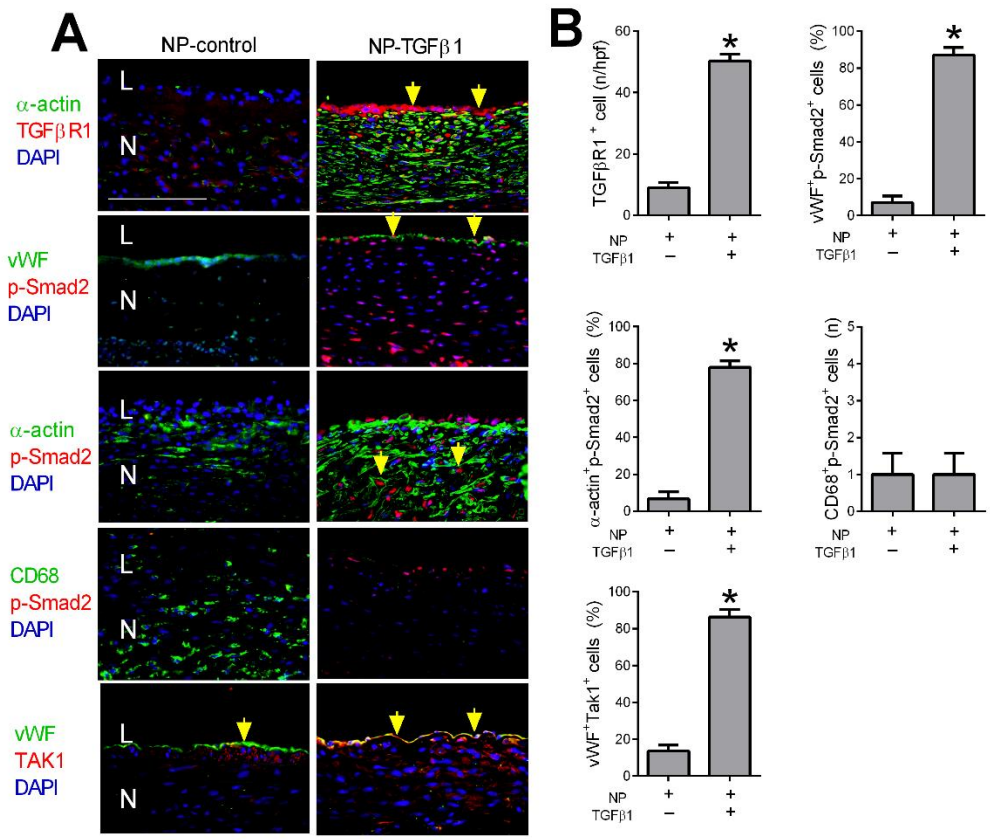

Supplementary Figure VI: Increased patch neointimal smad2 phosphorylation with TGFβ1 delivery. A) Immunofluorescence of the NP-control and NP-TGFβ1 groups, day 30; first row, merge of TGFβR1 (red), α-actin (green) and DAPI (blue); second row, merge of vWF (green), p-smad2 (green) and DAPI (blue); third row, merge of α-actin (green), p-smad2 (red) and DAPI (blue); fourth row, merge of CD68 (green), p-smad2 (red) and DAPI (blue); fifth row, merge of vWF (green), TAK1 (red) and DAPI (blue); L, lumen; N, neointima; yellow arrows show the dual positive cells; scale bar, 100 μm; n=3. **B)** Bar graphs showing TGFβR1 positive cells in the neointima (*, p=0.0001; t-test); vWF-pSmad2 dual positive cells in the neointima (*, p=0.0001; t-test); α-actin-pSmad2 dual positive cells in the neointima (*, p=0.0018; t-test); CD68-pSmad2 dual positive cells in the neointima (*, p>0.9; t-test); vWF-TAK1 dual positive cells in the neointima (*, p=0.0002; t-test). n=3.

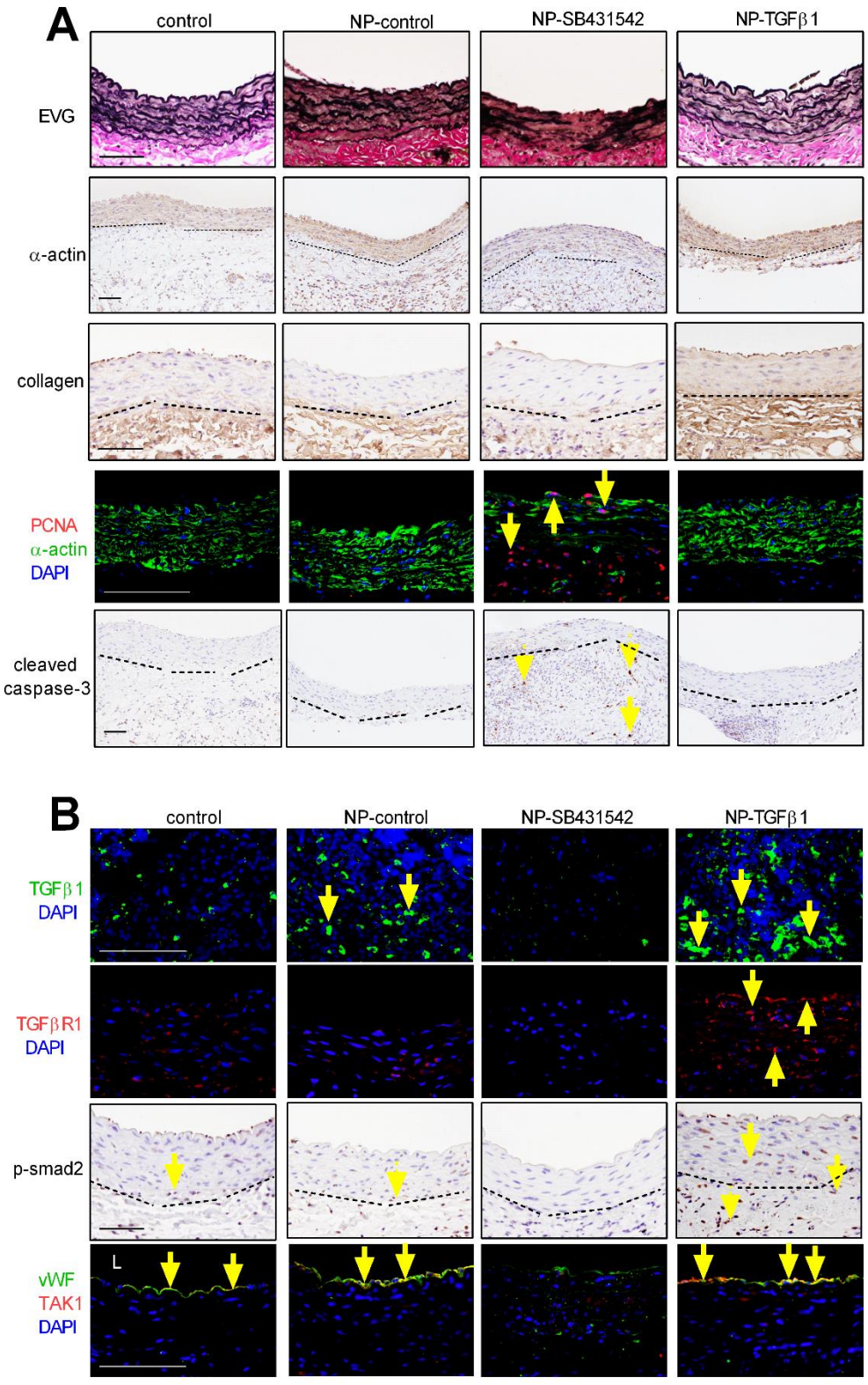

Supplementary Figure VII: Histology staining and TGFβ signaling with TGFβ1 inhibition. A) Immunofluorescence and immunohistochemistry showing the aorta wall in control, NP-control, NP-SB431542 and NP-TGFβ1 groups, day 7; First row, VVG staining; arrow shows break in

elastin fibers; second row, immunohistochemistry of α-actin; third row, immunohistochemistry of collagen; fourth row, merge of PCNA (red), α-actin (green) and DAPI (blue); fifth, immunohistochemistry stained with cleaved caspase-3; yellow arrows indicate positive cells; dashed line shows the demarcation of the media and adventitia; scale bar, 100 μm; n=3. **B)** First row, immunofluorescence of TGFβ1 (green) and DAPI (blue); second row, immunofluorescence of TGFβR1 (red) and DAPI (blue); third row, immunohistochemistry of p-smad2; fourth row, merged pictures of vWF (green), TAK1 (red) and DAPI (blue); L, lumen; yellow arrows show positive or dual positive cells; dashed line shows the demarcation of the media and adventitia; scale bar, 100 μm; n=3.

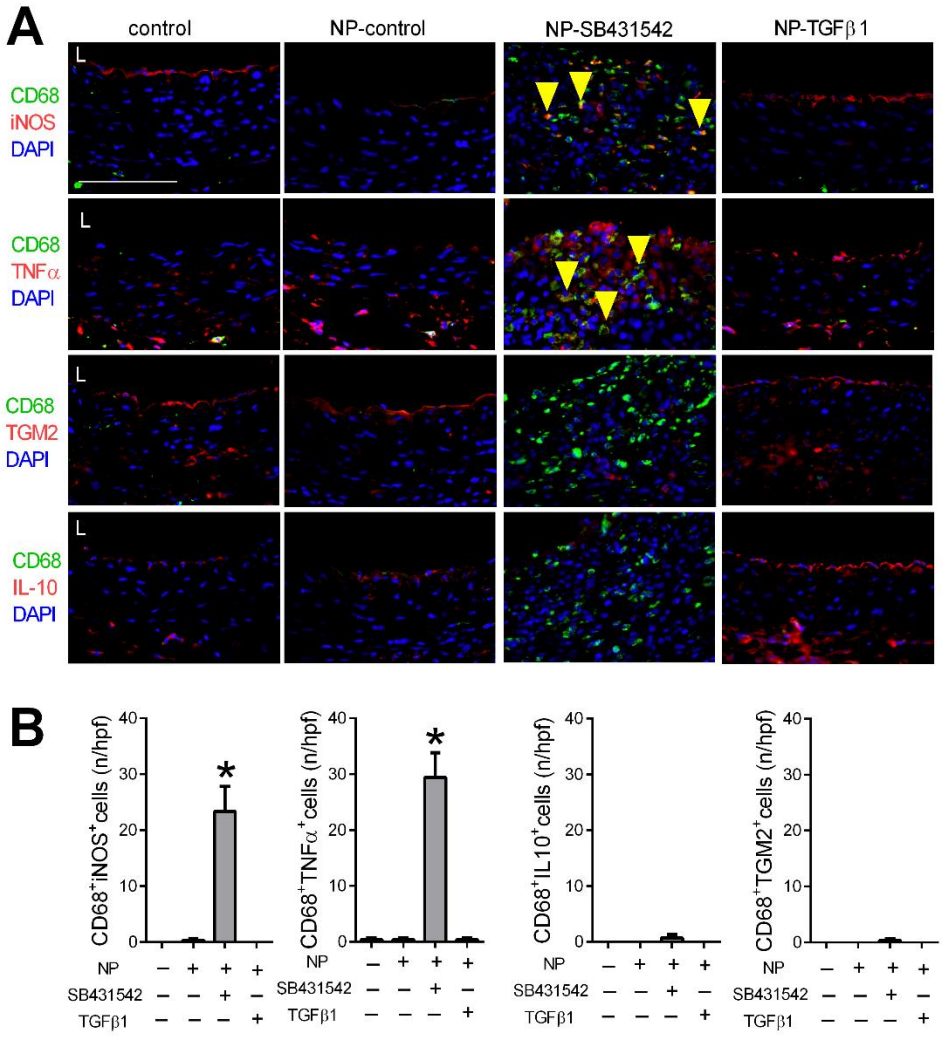

Supplementary figure VIII: Increased M1 type macrophages with TGFβ1 inhibition. A) Immunofluorescence analysis of the vessel wall after rat aorta patch angioplasty, day 7; first row, merge of CD68 (green), iNOS (red) and DAPI (blue); second row, merge of CD68 (green), TNFα (red) and DAPI (blue); third row, merge of CD68 (green), TGM2 (red) and DAPI (blue); fourth row, merge of CD68 (green), IL10 (red) and DAPI (blue); L, lumen; yellow arrowheads show the dual positive cells; scale bar, 100 µm; n=3. **B)** Bar graphs showing CD68 and iNOS dual positive cells (p=0.0002, ANOVA; *, p<0.0004, Tukey's multiple comparisons test); CD68 and TNFα dual positive cells (p<0.0001, ANOVA; *, p<0.0001, Tukey's multiple comparisons test); CD68 and TGM2 dual positive cells (p=0.4411, ANOVA); CD68 and IL10 dual positive cells (p=0.4411, ANOVA); n=3.

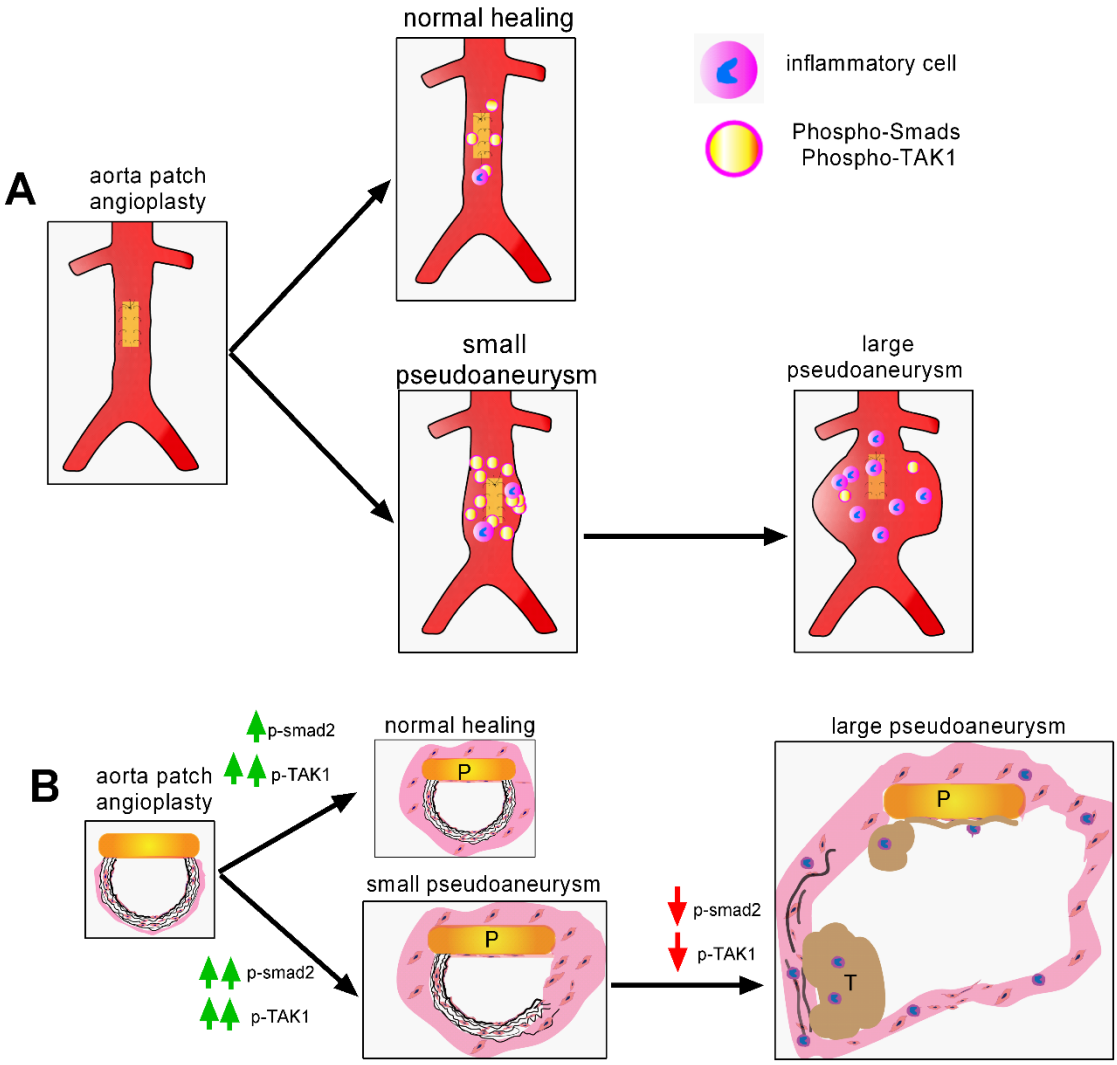

Supplementary Figure IX. Proposed mechanism of pseudoaneurysm formation after patch angioplasty. A) After patch angioplasty, normal healing is characterized by accumulation of inflammatory cells as well as some smad2-positive and TAK1-positive cells. **B)** Schematic diagram of pseudoaneurysm formation; P, patch; T, thrombus.
Activation of TGFβ1 signaling restricts wall degeneration to allow normal healing or formation of only a small pseudoaneurysm; decreased TGFβ1 signaling promotes formation of a large pseudoaneurysm.